Acta Biomaterialia 10 (2014) 2455–2462

Contents lists available at ScienceDirect

Acta Biomaterialia

journal homepage: www.elsevier.com/locate/actabiomat

Surface topography and chemistry shape cellular behavior on wide band-gap semiconductors

Lauren E. Bain [a], Ramon Collazo [b], Shu-han Hsu [c], Nicole Pfiester Latham [d], Michael J. Manfra [c,d,e], Albena Ivanisevic [a,b,*]

[a] UNC/NCSU Joint Department of Biomedical Engineering, North Carolina State University, Raleigh, NC 27606, USA
[b] Department of Materials Science and Engineering, North Carolina State University, Raleigh, NC 27606, USA
[c] Birck Nanotechnology Center, School of Materials Engineering, Purdue University, West Lafayette, IN 47907, USA
[d] Department of Physics, Purdue University, West Lafayette, IN 47907, USA
[e] School of Electrical and Computer Engineering, Purdue University, West Lafayette, IN 47907, USA

ARTICLE INFO

Article history:
Received 18 November 2013
Received in revised form 17 January 2014
Accepted 21 February 2014
Available online 28 February 2014

Keywords:
Gallium nitride
Rat pheochromocytoma (PC12) cells
Surface topography
Surface chemistry
Cell differentiation

ABSTRACT

The chemical stability and electrical properties of gallium nitride make it a promising material for the development of biocompatible electronics, a range of devices including biosensors as well as interfaces for probing and controlling cellular growth and signaling. To improve the interface formed between the probe material and the cell or biosystem, surface topography and chemistry can be applied to modify the ways in which the device interacts with its environment. PC12 cells are cultured on as-grown planar, unidirectionally polished, etched nanoporous and nanowire GaN surfaces with and without a physisorbed peptide sequence that promotes cell adhesion. While cells demonstrate preferential adhesion to roughened surfaces over as-grown flat surfaces, the topography of that roughness also influences the morphology of cellular adhesion and differentiation in neurotypic cells. Addition of the peptide sequence generally contributes further to cellular adhesion and promotes development of stereotypic long, thin neurite outgrowths over alternate morphologies. The dependence of cell behavior on both the topographic morphology and surface chemistry is thus demonstrated, providing further evidence for the importance of surface modification for modulating bio-inorganic interfaces.

1. Introduction

The preferential adhesion of cells to topographically roughened surfaces is a well-documented phenomenon [1–4], and can be considered in the context of the wide range of physical structures presented by the extracellular matrix (ECM) during development. These structures differ based on the functional role of the tissue under consideration, and the "ideal" surface for motivating maximal cell growth and viability generally bears structural and mechanical similarity to the tissue from which that cell line is derived [5–7]. Recent advancements in tissue engineering and implant design have taken advantage of this observation, with the preparation of more biomimetic surfaces involving addition of a micro- or nanotexture to the substrate or device surface [8]. Cells are exquisitely sensitive to a wide range of stimuli provided by their surroundings; in addition to this topographic sensitivity [9–11], cells are known to respond to mechanical forces [12–15], electric fields [16–18] and – perhaps the most thoroughly investigated – chemical cues [19–21]. These factors have been extensively studied in isolation; however, there are fewer resources documenting the combined effect of multiple factors in a specific, well-defined manner. Given the complex roles of these multiple stimuli in controlling cellular adhesion and differentiation, performing such combinatorial studies is integral for elucidating the mechanisms involved in cell development.

The conventional cell culture technique involves the seeding of cells on a flat planar surface, typically either glass or plastic. As the literature on and understanding of mechanobiology has expanded, however, the importance of micro- and nanoscale surface topographies for promoting specific cellular behaviors has been established. Identification of the features that drive said behaviors is a factor of importance for tissue engineering; as an example, stem cell differentiation can be guided solely by changing the roughness and elasticity of a surface, with cells taking on characteristics of the tissues with comparable properties [5,12,22]. In addition to

* Corresponding author at: Department of Materials Science and Engineering, North Carolina State University, Raleigh, NC 27606, USA. Tel.: +1 919 515 4683.
E-mail address: Ivanisevic@ncsu.edu (A. Ivanisevic).

http://dx.doi.org/10.1016/j.actbio.2014.02.038
1742-7061/

straightforward variation in roughness, neural cell growth is demonstrably different on ordered vs. disordered arrays of electrospun poly(ε-caprolactone) (PCL) nanofibers generated under otherwise identical conditions [23]. While the exact change in behavior due to topography depends on cell type, this represents a path through which surfaces of comparable surface roughness but variable topography can be used to influence cell growth.

Neural cells are of particular interest in considering the applications of semiconductor materials for interfacing biosystems [24]. The axonal growth cone is particularly sensitive to external stimuli, and the prominent neurite extensions provide a distinct means of assessing changes to cell response [25]. Rat pheochromocytoma (PC12) cells are a well-established model system for neurons that differentiate upon exposure to nerve growth factor (NGF) [26–28]. PC12 cell sensitivity to nanoscale structures has been confirmed on nanoscale ridges between 70 and 250 nm in width [29], and previous studies have also assessed the role of a laminin-derived peptide motif in improving PC12 cell adhesion to a semiconductor surface [30,31]. The semiconductor used in these studies, gallium nitride (GaN), has emerged as a compelling semiconductor material for interfacing with cells. Its biocompatibility [31–33], chemical stability [34] and electrical performance in ionic solutions [35] all point to the potential of GaN for developing functional devices for probing cells and biosystems. GaN has been extensively studied by the photonics community, and processes for generating nanopores [36,37] or nanowires [38,39] have been developed to improve emission characteristics for optoelectronic applications. Chemical modification schemes featuring both covalent functionalization [40,41] and identification of recognition peptides that demonstrate specific adhesion to the GaN surface [34,42] have also been established. The existence of topographic and chemical modification schemes, in addition to the known favorable electrical and optical properties of GaN, provide compelling reasons to study the potential of GaN for interfacing with biological tissues and systems.

An important factor to consider with the recent boom in research coupling engineered nanostructures with biomolecules and biological environments is the dynamics of proteins interacting with the engineered surfaces. Nanoscale topographic modification has become more widespread as researchers continue evaluating the dynamics of cell–nanostructure interactions [43–46]. Semiconductor nanostructures have attracted a great deal of interest as materials for field effect transistor-based biosensors, as the reduction in bulk material allows a significantly smaller quantity of analyte to elicit the same degree of change observed in a planar bulk device [47] With the expanding interest in nanostructure-based devices, it is increasingly important to evaluate the dynamics of interaction between biomolecules and nanostructured or nanotextured materials. Development of nanoscale roughened surface morphologies on GaN can have a significant effect on the water contact angle [48], with potential implications as to the wetting behavior observed when exposed to physiologic solutions and subsequent interaction between soluble proteins and the GaN surface. Local variations in surface curvature have also been demonstrated to influence the orientation of laminin, a protein associated with cell adhesion, adsorbed to the surface [49]. Given the general sensitivity of cell membrane receptors to the structure and conformation of proteins, this could have significant effects on subsequent cell–surface interactions. Contradictory to these results, however, are those suggesting that nanometer scale roughness does not influence the amount or structure of protein on a surface [50] or that the only changes in quantity of adsorbed protein relates to the change in surface area brought on by increasing roughness [51]. Further exploration of the interactions between surface nanostructures and biomolecules will provide settlement to this discrepancy.

This study brings together both the nanoscale topographic modification of a semiconductor material and chemical modification by introduction of the isoleucine–lysine–valine–alanine–valine (IKVAV) motif, a core peptide domain of laminin. The IKVAV motif can play a role in neural adhesion and differentiation, and has been used to treat surfaces in schemes involving both physisorption and covalent modification [30]. By evaluating the combined effect of topography and chemistry, the effects of nanostructured GaN topography on both PC12 cell development and IKVAV peptide physisorption are catalogued.

2. Materials and methods

Chemicals were ordered from Sigma Aldrich unless otherwise specified. Rat pheochromocytoma (PC12) cells were purchased from ATCC (Manassas, VA). Type I Rat Tail Collagen was purchased from BD Biosciences (San Jose, CA). Dulbecco's modified Eagle's medium (DMEM), high-glucose formulation, fetal bovine serum, horse serum, 0.5% trypsin-ethylenediaminetetraacetic acid, murine nerve growth factor and penicillin–streptomycin were purchased from Invitrogen (Grand Island, NY). The peptide sequence (referred to in the text by the primary motif, "IKVAV") was a 19-amino acid sequence, CSRARKQAASIKVAVSADR, purchased from GenScript (Piscataway, NJ).

2.1. GaN template preparation

2.1.1. GaN growth

The gallium nitride template consisted of an unintentionally doped, 1 μm thick, gallium polar gallium nitride film grown on c-plane sapphire by metalorganic chemical vapor deposition and exhibiting a smooth morphology [52]. The film was grown on a high temperature AlN layer grown on a low temperature AlN nucleation layer to control polarity. This structure yielded a gallium nitride film with a dislocation density of 1×10^9 cm^{-2}. The chosen growth conditions, in addition to the low sapphire substrate miscut, yielded a surface morphology dominated by growth spirals arising from screw dislocations intersecting the growing surface.

Polished substrates were generated using a mechanical polishing wheel with 6 μm diamond slurry (Buehler METADI). Porous substrates were generated using an electroless wet chemical etch [36]. Briefly, surfaces were cleaned using HNO_3 prior to sputter coating with Pt islands, 1 mm in diameter. Pt-decorated surfaces were etched in a solution of 1:2:1 38% H_2O_2, 49% HF and methanol for 1 h under a 100 W UV lamp. Multiple rinses in methanol and deionized water were used to remove etch residue.

2.1.2. GaN NW growth

Samples were grown on Si(1 1 1) by plasma assisted molecular beam epitaxy (PAMBE). Prior to loading into the MBE, the Si substrates were cleaned by ultrasonication in acetone, methanol and isopropanol, each for 10 min, and treated with buffer oxide etch. Before growth, the substrates were outgassed at 905 °C. Temperature readings were taken with a pyrometer. The appearance of the 1×1 reflection high energy electron pattern at 905 °C, as well as the 7×7 pattern at temperatures lower than 830 °C, ensured the cleanliness of the samples. The RF plasma power was 405 W with a nitrogen flow rate of 1.3 sccm. The beam equivalent pressure for Ga was 2.9×10^{-8} torr, resulting in a III/V ratio of 0.16. We employed a two-step growth process. The two-step growth process had an initial nucleation temperature of 790 °C for 22.5 min, followed by a growth time of 12 h at 825 °C.

For cell culture experiments, samples were sonicated 15 min each in acetone, ethanol and deionized water. Surface cleaning

was performed by a 5 min etch in piranha (3:1 sulfuric acid to hydrogen peroxide), followed by a 10 min etch in HCl to remove surface hydroxyl groups introduced by the piranha solution. Samples were rinsed with deionized water and dried with N_2. Immediately prior to cell culture, samples were dipped in 70% ethanol and either exposed to UV light in the cell culture cabinet for 30 min or placed in the peptide incubation solution. Samples, 3 mm × 3 mm in size, were incubated in a 10 μl droplet of 0.1 mM peptide for 21 h in the refrigerator in a sealed chamber; the volume used for the nanowire substrate was substantially increased (4 ml) to both accommodate the increased surface area and overcome the surface hydrophobicity. Following removal from the incubation solution, samples were rinsed with PBS and dried with N_2 prior to UV exposure for 30 min in the cell culture cabinet. The power and duration are not expected to damage or degrade the peptide treatment (as discussed by Jewett et al. [31].)

2.2. Cell culture

Culture medium for PC12 cells consisted of DMEM with 12.5% horse serum, 2.5% fetal bovine serum and 1% penicillin/streptomycin. Cells were kept in an incubator held at 37 °C and 5% CO_2. Cells were passaged either once or twice after thawing prior to seeding on the GaN substrates. Three or more replicates of each type of substrate, with the exception of the nanowires, were placed in collagen-coated 24-well plates (one substrate per well). Generally, for a meaningful analysis, a population of $n > 100$ cells for each condition is counted. While cell populations were adequate with three repeats for the IKVAV-modified surfaces, the unmodified surfaces required additional substrates to attain adequate cell populations. This is accounted for in the statistical analysis (see Section 2.4 for more details). One nanowire substrate was used for each surface chemistry – unmodified and IKVAV-treated – and wafers were placed in a collagen-coated 60 mm well plate for each experiment. Cells were seeded at low density (4×10^4 cells ml^{-1}) to allow observation of any neuritic connections formed following nerve growth factor (NGF) exposure. After seeding, cells were given 12 h to adhere prior to replacement of the standard culture medium with DMEM containing 1% horse serum and 50 ng ml^{-1} NGF. This NGF medium was replaced after 3 days of culture, and cells were fixed using Trump's 4F:1G fixative [53] on day 6. Cells were then dehydrated via a graded ethanol series followed by critical point drying and sputter coating with Au/Pd for scanning electron microscopy (SEM).

2.3. Microscopy

Optical micrographs were collected using an Olympus BH2-UMA microscope with a Zeiss Axiocam camera at day 6 of cell culture on the GaN substrates. Images were processed using ImageJ software. Optical images were used to compile adherent cell density data. Nine images were used to make a composite for each 3 × 3 mm^2 substrate, and adherent cell density was calculated on a substrate-by-substrate basis. Adherent cell densities for the nanowire substrates were compiled from ten images taken at random positions on the substrate.

Scanning electron micrographs were collected using a Jeol JSM-6010LA scanning electron microscope. All cell images were collected with a 5 or 10 kV beam. Images were processed and false colored using ImageJ. Enough images were collected to achieve a cell population of at least 100 analyzed cells. Differentiation counts were performed three times to verify consistency of phenotype identification; values are reported as an average of three counts, with their associated standard deviation. Statistical analysis was performed on the basis of the triplicate counts.

Root-mean-square (RMS) roughness data were collected using a Cypher atomic force microscope (Asylum Research, Santa Barbara, CA). For this, 5 × 5 and 30 × 30 μm^2 images at a 1024 × 1024 resolution were collected in tapping mode with a scan rate of 1 Hz. Five images were collected from each of three samples for each surface topography.

2.4. Statistical analysis

Statistical analysis was performed using SAS statistical analysis software (SAS Institute, Cary, NC). The general linearized model (GLM) for performing analysis of variance (ANOVA) on unbalanced data was used to analyze cell density data; this process accommodates unbalanced data sets, in this case the unequal number of substrates used for density analysis. A Tukey–Kramer adjustment of the least squares means with a significance level of 0.05% ($\alpha = 0.05$) was used following GLM assessment to establish significance. A two-sided ANOVA with a significance level of 0.05% ($\alpha = 0.05$) was used to compare between topographies and chemical modifications. A one-sided ANOVA followed by Tukey–Kramer adjustment, again with a 0.05% significance level, was used to compare contact angles and roughness values of the prepared GaN surfaces.

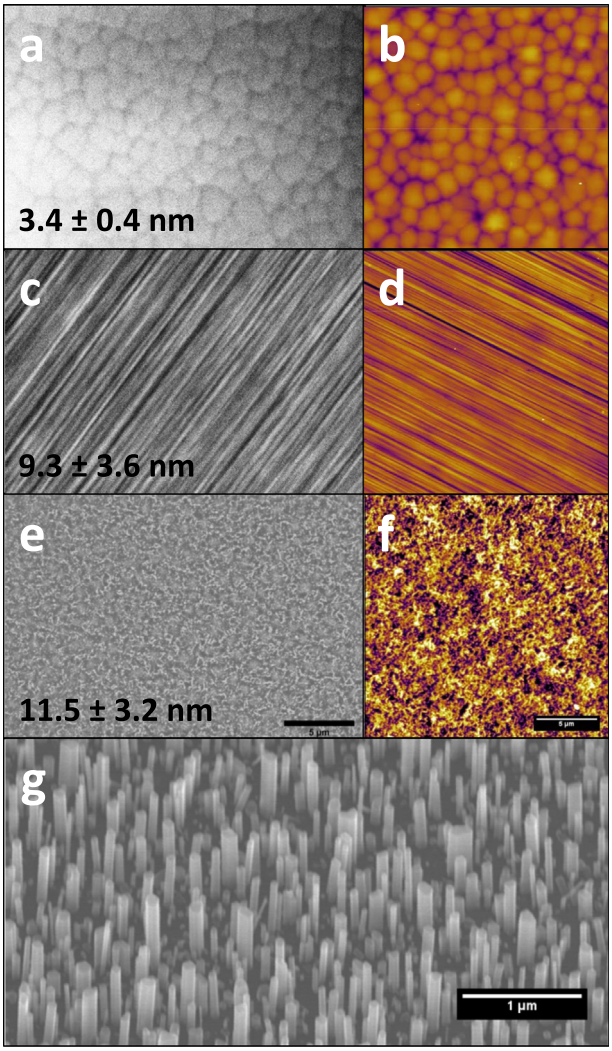

Fig. 1. Planar (a and b), polished (c and d) and etched (e and f) GaN surfaces. (a, c, e and g) Scanning electron micrographs and (b, d and f) AFM height profiles display the morphology of the prepared surfaces. RMS roughness values are listed at the bottom left of the SEM images. (g) The nanowire substrate, taken at an angle to better depict the nanowire aspect ratios.

3. Results

3.1. Characterization of GaN surfaces

The three primary surfaces studied – planar, etched and polished GaN – were initially characterized using atomic force microscopy (AFM) and SEM. Characterization of the nanowire (NW) substrates was limited to SEM due to the high aspect ratios of the nanostructures which prevented the collection of useful AFM data. Fig. 1 provides plan-view electron micrographs and matched-scale images taken from the AFM data, providing clear observation of the surface topographies. Corresponding surface roughness values are available for the three surface studied using AFM. Values are 3.4 ± 0.4 nm for the planar surface, 9.3 ± 3.6 for the polished surface and 11.5 ± 3.2 for the etched surface. As stated, the planar samples are not atomically flat; however, in the context of the experiment they are representative of an as-grown flat surface, and are thus designated "planar" for the remaining discussion. There is no statistical significance between the polished and etched surface according to Tukey's studentized range test. While the planar and NW surfaces present the flat and maximally rough surfaces for this study, the compelling comparison is thus between the polished and etched cases. The surface RMS roughness values are statistically similar, but the morphology of that roughness is markedly different – unidirectional features in contrast to a more random texture. This also manifests as a significant change in contact angle, shown in Fig. 2. As can be seen in the droplet profiles, wetting behavior shifts to the more hydrophilic regime for the polished surfaces and to the more hydrophobic regime for the porous surface.

Chemical variation in the surfaces due to the surface treatments is a general concern. To confirm chemical similarity of the surfaces, Raman spectroscopy was performed. There were no noticeable differences in the Raman spectra (data available in the Supplementary information; Fig. S1); thus, any residue associated with polishing, etching, or nanowire growth is assumed to be insignificant.

3.2. Cell adhesion on topographically and chemically modified GaN

In keeping with the expected results for increased surface roughness [1], the density of adherent cells on chemically unmodified surfaces increased with RMS roughness, as shown in Fig. 3. The optical micrographs from which these data were derived are presented in the Supplementary information see Fig. S2. The particularly impressive density observed on the nanowires, however, is attributed to the increased well-plate surface area occupied by the GaN sample. As cells are introduced to the wells, they drop to the bottom and adhere to either the GaN sample or the collagen-coated well, depending on location. A larger number of cells were also introduced to the NW well; the working volume for the culture vessel used is 5 ml, whereas a 24-well plate has a working volume of 0.5 ml per well. Cells were introduced at a density of 4×10^4 cells ml^{-1}; the combination of a greater number of added cells and an increased surface area fraction of the total culture environment is likely responsible for this significant response.

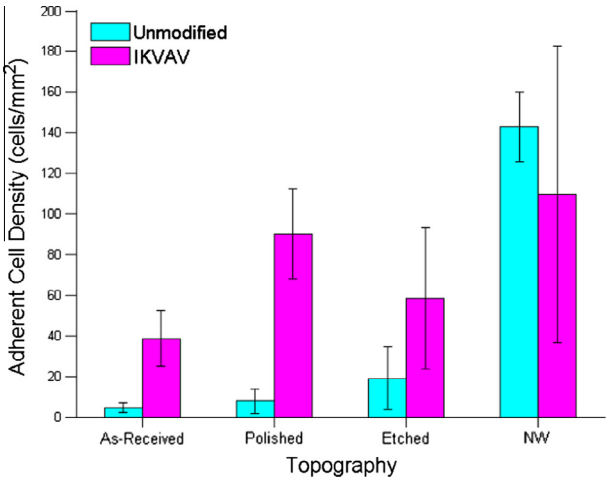

Fig. 3. Adherent cell density by substrate. As expected, surface roughness inspires increased adherent cell densities. Modification with the IKVAV motif generally increases the density of adherent cells ($p < 0.05$, two-sided ANOVA, Tukey–Kramer adjustment for multiple comparisons), although the effect on the nanowire surface is limited. The extent of the change inspired by IKVAV modification also varies with topography.

One of the more significant changes is then in the response to modification via incubation with the IKVAV-containing peptide sequence. With the exception of the NW surface, IKVAV increases cell adhesion in all cases, with the greatest increase taking place on the polished surface. Morphological responses to IKVAV are also significant. Fig. 4 demonstrates representative cell growth on the four surfaces in the unmodified state, while Fig. 5 provides representative images of cells grown on IKVAV-modified surfaces. The most significant morphological change with IKVAV treatment occurs

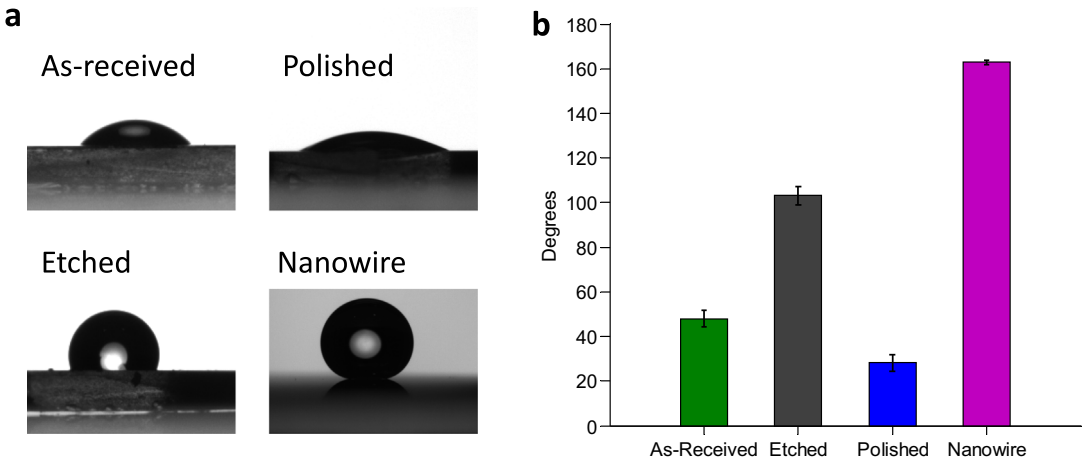

Fig. 2. Contact angle images (a) and values (b) for the prepared surfaces. The nanowires present superhydrophobic behavior, as expected for their topographic profile. The reduced contact angle of the polished substrate is indicative of the unidirectional grooves facilitating droplet spread over the surface. All values are statistically significant from one another (Tukey's studentized range procedure, $\alpha = 0.05$).

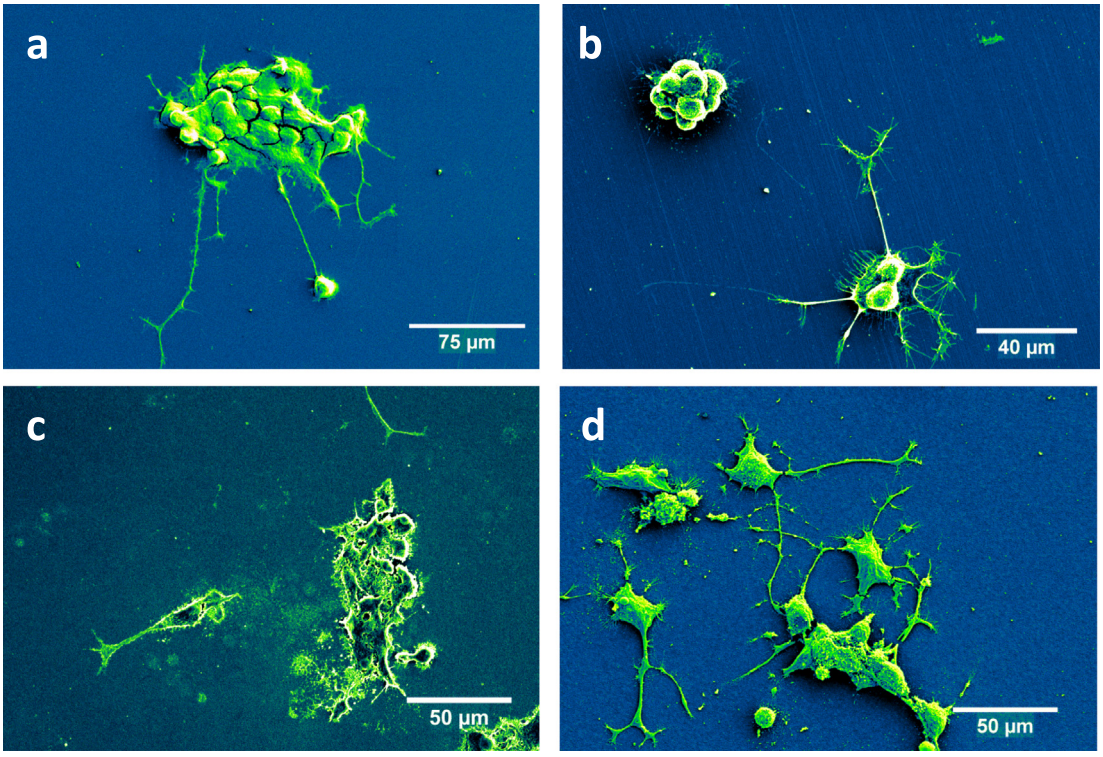

Fig. 4. Scanning electron micrographs of cells on chemically unmodified GaN surfaces representative of variations in cellular morphology: (a) planar, 75 μm scale bar, (b) polished, 40 μm scale bar, (c) etched and (d) NW topographies, 50 μm scale bars.

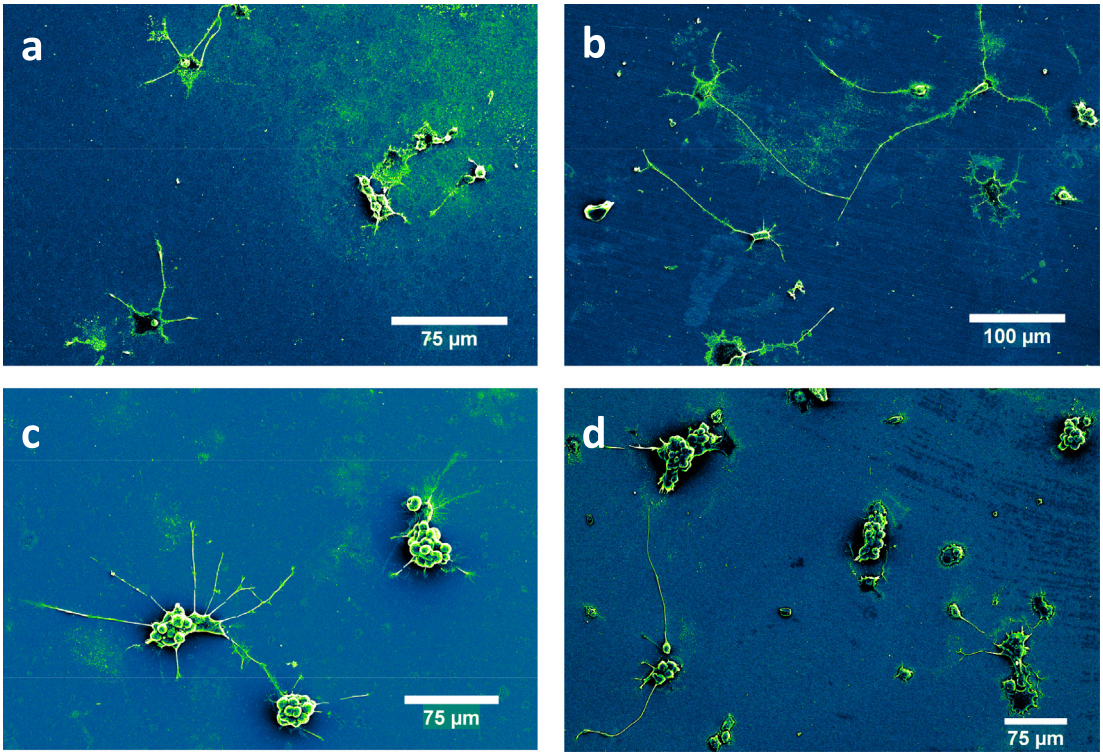

Fig. 5. Scanning electron micrographs of cells on GaN modified with the IKVAV motif, representative of variations in cellular morphology: (a) planar, 75 μm scale bar, (b) polished, 100 μm scale bar, (c) etched, 75 μm scale bar, and (d) NW, 75 μm scale bar. Images collected with an optical microscope (provided in the Supplementary information) depict the overall increase in adherent cell density.

on the etched surface; the number of cells differentiating with long, thin extensions increases drastically when the surface has been treated with IKVAV.

To quantify the change in morphology, three phenotypes of morphological characteristics were established. Cells were first identified as either having differentiated or not, with a lack of

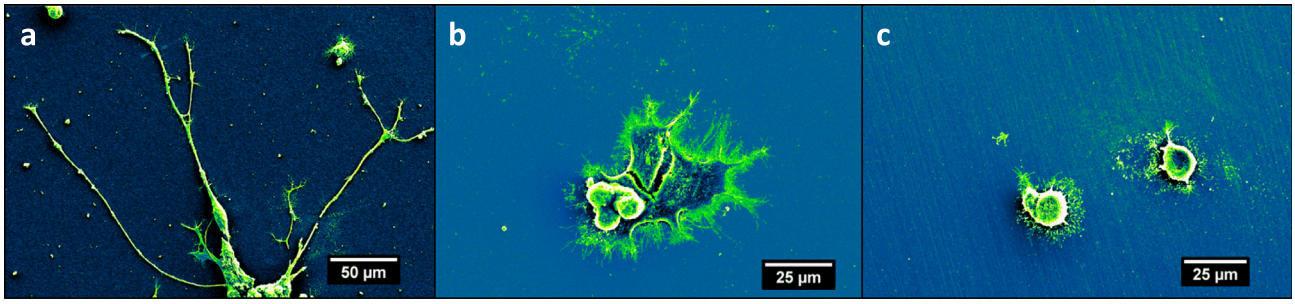

Fig. 6. Representative examples of the established morphological characteristics: (a) long, thin neuritic extensions, 50 μm scale bar: (b) flattened, spread cell body, with a small clump of three non-differentiated cells on top, 25 μm scale bar; (c) non-differentiated cells, 25 μm scale bar.

differentiation indicated by the cells retaining a standard round morphology associated with PC12 cells prior to NGF exposure. The concentration of NGF used for the experiment is described as having a half-maximal effect; thus, we do not expect 100% of the cell population to demonstrate differentiation. Differentiated cells can then be divided into two prominent morphologies: those having long, thin extensions, where the width of the extension is less than 20% of the cell body and the length is greater than the length of the cell body; and those having flattened, spread features, where the cell body is no longer circular in shape, spread area is at least double that of the average non-differentiated cell and extensions, if present, are greater than 20% of an average non-differentiated cell body in width. Fig. 6 provides clarification on these phenotypes; Fig. 6a has several examples of cells having thin extensions, while Fig. 6b provides a flat, spread cell with non-differentiated cells clustered on top. Fig. 6c reveals more isolated non-differentiated cells; while one exhibits small extensions, these are not substantial enough to qualify as being differentiated cells.

Using this basis for identifying cells, the relative populations of differentiated cells were then assessed. Initial consideration was given to the ability of topography or surface treatment to motivate differentiation; results displaying the percentage of differentiated cells of either morphology are provided in Fig. 7. Polished and etched surfaces demonstrate higher populations of differentiated cells without IKVAV treatment; however, there is a reduction in the relative population of differentiated cells with the addition of peptide. It is also of interest to explore the specific morphology

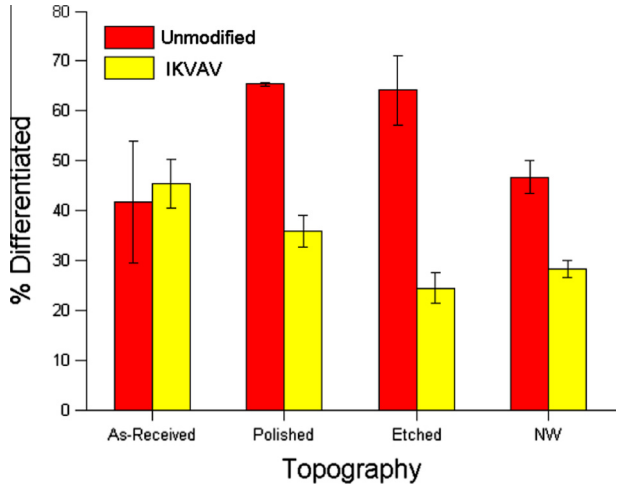

Fig. 7. Percentage of differentiated cells by substrate, with and without IKVAV treatment. There is no significant difference in the unmodified and IKVAV values for the AR surface. The unmodified polished and etched surfaces are distinct from the AR and NW surfaces, but are not statistically distinguishable from each other.

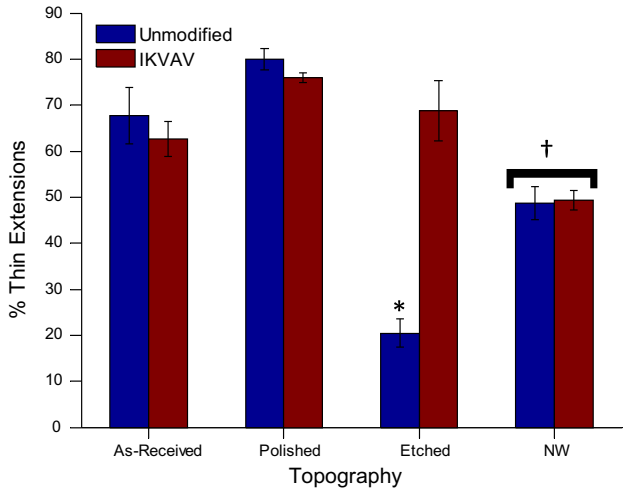

Fig. 8. Of the population of differentiated cells, the percentage expressing the long, thin extension phenotype. Symbols (* and †) designate statistically significant differences in values.

of the differentiated cells. For the specific subset of the cell population expressing differentiation, Fig. 8 provides the percentage of cells expressing the thin neuritic extension phenotype. The most significant change is in the etched surface, which also demonstrated the lowest percentage of cells expressing the stereotypic neurite extensions prior to surface treatment. IKVAV treatment reverses this influence, returning the number of cells with thin extensions to a level comparable to the polished and planar surfaces. Cell phenotypic demographics remained largely the same for the NW surface.

4. Discussion

Cell response to physical topography is an exceedingly well established phenomenon, with initial investigations taking place during the early twentieth century [8,11,54–56]. While the improvement in cellular adhesion with the introduction of substrate roughness is not a surprise, the use of semiconductors and established processing methods for photonic devices introduces a new scheme for generating nanometer-scale roughness.

4.1. Topography and cell morphology

In the context of this experiment, the AR and NW surfaces represent the limits of surface roughness – a flat GaN surface, and a "maximally rough" surface of high aspect ratio features. It is thus worthwhile to consider the two mid-tier surfaces in the context

of behaviors observed on this "flat" and "maximally rough" surface. The etched surface resembles the NW in that the texture is disordered; there is no uniform alignment. The polished surface, by contrast, has aligned surface features; while the RMS roughness values are approximately equal, the surface morphology demonstrates significant differences. This is fairly unique in the context of available literature; while many works document the effects of ridges and grooves of different dimensions on cell growth [56,57], there are fewer resources exploring the effect of variable morphologies with consistent roughness.

Comparing growth on the unmodified surfaces produces a compelling result with respect to cellular morphology. As shown in Fig. 8, the majority of the differentiated cell population on the polished surfaces exhibits the stereotypic long, thin extensions associated with neuronal development. In contrast, the etched surface demonstrates a much greater extent of cell spreading. In the context of filopodial interactions with the surface and contact guidance [11,25], this is an expected behavior – the unidirectional features of the polished surface provide troughs along which neurites can extend, with barriers on either side. By contrast, the etched surface has a more random distribution of surface features; rather than a continuous ridge for cell extensions to "follow", the cells are left with a wider range of contact points, providing an explanation for the likelihood of cell spreading and lack of organized neurite formation.

The etched surface also features the most compelling morphological change when modified with the IKVAV peptide motif – the differentiation behavior reverses, and the number of cells with long, thin extensions more closely resembles that of the planar and polished surfaces. To explain this change, the role of laminins and the IKVAV motif can be evaluated. In addition to motivating cellular adhesion to the basal lamina, the IKVAV motif is associated with neuronal development. While two phenotypes of differentiation are observed here for PC12 cells, the conventional exhibition of differentiation is the stereotypical thin neuritic axon. Thus, it is likely that addition of the IKVAV motif is able to more strictly regulate the nature of cellular differentiation than topography alone, promoting the expected neuronal behavior over the alternate spread morphology observed on the unmodified etched surface. The functional role of IKVAV in cell adhesion may also contribute to the decrease in the percentage of differentiated cells observed in Fig. 7. Synthetic analogs to IKVAV with replacement of different residues have maintained their ability to promote cell adhesion, but upon replacement of the lysine or isoleucine residues the sequence fails to promote neurite outgrowth [58]. Given the reduction in differentiated percentage with an increase in population, the results reported here suggest that addition of the IKVAV sequence is more effective at promoting cellular adhesion than neurite outgrowth from PC12 cells in the context of this experiment.

4.2. Nanoscale topography and peptide physisorption

Physical topography has been implicated in the structural dynamics of protein adsorption to surfaces [49–51]. This observation, and the known sensitivity of cell membrane receptors to the conformation of their associated proteins, indicate the importance of tuning material surfaces to optimize the performance of any surface treatment. The influence of surface topography is evidenced by the magnitude of increase in cell density with IKVAV treatment across the four conditions. If topography did not play a role in peptide adsorption, the increase in adherent cell density would be constant across the surfaces; however, there are differences in the increased cell population, with the polished surface exhibiting a significant increase in density ($p < 0.02$ when comparing densities with and without IKVAV modification). This can be thought of in the context of wetting on the different surfaces. Recall the contact angle data presented in Fig. 2 – the polished surface has a significantly lower contact angle than the other surfaces, with a greater droplet spread and larger area of contact with the droplet. In the same way, during incubation, the peptide droplet during incubation spreads across the surface and is able to maximize the area of contact with the sample surface. While a comparable effect is expected for the planar surface, as this has yet to enter the hydrophobic regime, there is also an increase in surface area associated with the roughening of the polished surface. The results from the etched and NW surface also indicate an interesting wetting phenomenon – namely, introduction of the Cassie–Bennet condition. Wenzler wetting, as observed with the polished surface, involves the droplet coming into full contact with the surface, while Cassie–Bennet wetting is associated with a droplet resting on top of surface features with air filling in the interdigital space. The reduced increase (or total lack of increase, as observed in the NW case) in cell density is attributed to this lack of contact between the peptide solution and the full area of the substrate surface. A BCA assay was attempted to confirm; however, the resolution of the assay and spectrophotometric detection was inadequate to confirm any significant change among surfaces (Supplementary information, Fig. S3). The change in cellular behavior is still adequate to assert that IKVAV has adsorbed to the surface, and that the quantity of accessible IKVAV in cell–surface interactions differs by substrate.

5. Conclusion

This work in coupling physical topography and biochemical adsorption on a GaN substrate contributes to the body of work supporting the use of GaN for biocompatible electronic or photonic devices, as well as the importance of tuning surface properties when coupling nanoscale structures with biomolecules. While topographic modification is demonstrated to influence cell growth in a manner involving the morphology as well as roughness of a surface, the influence of topography on the adsorption of proteins or peptides to the surface must be considered when performing surface modification. These factors are not entirely distinct, and generation of functional bio-inorganic interfaces will rely on a complex understanding of the dynamics of the nanostructure–biomolecule interaction.

Acknowledgments

Dr. Susan Bernacki provided assistance in cell culture techniques and maintenance of cell culture facilities. Corey Foster, Dr. Scott Jewett and Dr. Matt Makowski provided guidance in cell culture techniques and working with gallium nitride in a cell culture environment.

Appendix A. Figures with essential colour discrimination

Certain figures in this article, particularly Figs. 1–8 are difficult to interpret in black and white. The full colour images can be found in the on-line version, at http://dx.doi.org/10.1016/j.actbio.2014.02.038.

Appendix B. Supplementary data

Supplementary data associated with this article can be found, in the online version, at http://dx.doi.org/10.1016/j.actbio.2014.02.038.

References

[1] Curtis A, Wilkinson C. Topographical control of cells. Biomaterials 1997;18:1573–83.
[2] Stevens MM, George JH. Exploring and engineering the cell surface interface. Science 2005;310:1135–8.
[3] Webster TJ, Ergun C, Doremus RH, Siegel RW, Bizios R. Specific proteins mediate enhanced osteoblast adhesion on nanophase ceramics. J Biomed Mater Res 2000;51:475–83.
[4] Miller DC, Thapa A, Haberstroh KM, Webster TJ. Endothelial and vascular smooth muscle cell function on poly(lactic-co-glycolic acid) with nano-structured surface features. Biomaterials 2004;25:53–61.
[5] Kingham E, White K, Gadegaard N, Dalby MJ, Oreffo ROC. Nanotopographical cues augment mesenchymal differentiation of human embryonic stem cells. Small 2013;9:2140–51.
[6] Georges PC, Janmey PA. Cell type-specific response to growth on soft materials. J Appl Phys 2005;98:1547–53.
[7] Engler AJ, Carag-Krieger C, Johnson CP, Raab M, Tang HY, Speicher DW, et al. Embryonic cardiomyocytes beat best on a matrix with heart-like elasticity: scar-like rigidity inhibits beating. J Cell Sci 2008;121:3794–802.
[8] Ratner BD, Bryant SJ. Biomaterials: where we have been and where we are going. Annu Rev Biomed Eng 2004;6:41–75.
[9] Dalby MJ, Riehle MO, Sutherland DS, Agheli H, Curtis ASG. Use of nanotopography to study mechanotransduction in fibroblasts – methods and perspectives. Eur J Cell Biol 2004;83:159–69.
[10] Dalby MJ, Riehle MO, Johnstone H, Affrossman S, Curtis ASG. Investigating the limits of filopodial sensing: a brief report using SEM to image the interaction between 10 nm high nano-topography and fibroblast filopodia. Cell Biol Int 2004;28:229–36.
[11] Hoffman-Kim D, Mitchel JA, Bellamkonda RV. Topography, cell response, and nerve regeneration. In: Yarmush ML, Duncan JS, Gray ML, editors. Annual Review of Biomedical Engineering, Vol. 122010. Annual Reviews. pp. 203–31.
[12] Rehfeldt F, Engler AJ, Eckhardt A, Ahmed F, Discher DE. Cell responses to the mechanochemical microenvironment – implications for regenerative medicine and drug delivery. Adv Drug Deliv Rev 2007;59:1329–39.
[13] Wang JHC, Thampatty BP. An introductory review of cell mechanobiology. Biomech Model Mechanobiol 2006;5:1–16.
[14] Wang JHC, Thampatty BP, Lin JS, Im HJ. Mechanoregulation of gene expression in fibroblasts. Gene 2007;391:1–15.
[15] Ingber DE. Mechanobiology and diseases of mechanotransduction. Ann Med 2003;35:564–77.
[16] Nedergaard M. Direct signaling from astrocytes to neurons in cultures of mammalian brain-cells. Science 1994;263:1768–71.
[17] Hinkle L, McCaig CD, Robinson KR. The direction of growth of differentiating neurons and myoblasts from frog embryos in an applied electric-field. J Physiol Lond 1981;314:121.
[18] Aaron RK, Boyan BD, Ciombor DM, Schwartz Z, Simon BJ. Stimulation of growth factor synthesis by electric and electromagnetic fields. Clin Orthop Relat Res 2004:30–7.
[19] Baggiolini M. Chemokines and leukocyte traffic. Nature 1998;392:565–8.
[20] Ridley AJ, Schwartz MA, Burridge K, Firtel RA, Ginsberg MH, Borisy G, et al. Cell migration: integrating signals from front to back. Science 2003;302:1704–9.
[21] Cuchiaraa ML, Hortera KL, Bandaa OA, West JL. Covalent immobilization of stem cell factor and stromal derived factor 1α for in vitro culture of hematopoietic progenitor cells. Acta Biomater 2013;9:9258–69.
[22] Higuchi A, Ling QD, Chang Y, Hsu ST, Umezawa A. Physical cues of biomaterials guide stem cell differentiation fate. Chem Rev 2013;113:3297–328.
[23] Xie J, MacEwan MR, Li X, Sakiyama-Elbert SE, Xia Y. Neurite outgrowth on nanofiber scaffolds with different orders, structures, and surface properties. ACS Nano 2009;3:1151–9.
[24] He QY, Sudibya HG, Yin ZY, Wu SX, Li H, Boey F, et al. Centimeter-long and large-scale micropatterns of reduced graphene oxide films: fabrication and sensing applications. ACS Nano 2010;4:3201–8.
[25] Dent EW, Gupton SL, Gertler FB. The growth cone cytoskeleton in axon outgrowth and guidance. Cold Spring Harb Perspect Biol 2011;3.
[26] Greene LA, Tischler AS. Establishment of a noradrenergic clonal line of rat adrenal pheochromocytoma cells which respond to nerve growth-factor. Proc Natl Acad Sci USA 1976;73:2424–8.
[27] Connolly JL, Greene LA, Viscarello RR, Riley WD. Rapid, sequential changes in surface morphology of PC12 pheochromocytoma cells in response to nerve growth factor. J Cell Biol 1979;82:820–7.
[28] Gottlieb PA, Barone T, Sachs F, Plunkett R. Neurite outgrowth from PC12 cells is enhanced by an inhibitor of mechanical channels. Neurosci Lett 2010;481:115–9.
[29] Foley JD, Grunwald EW, Nealey PF, Murphy CJ. Cooperative modulation of neuritogenesis by PC12 cells by topography and nerve growth factor. Biomaterials 2005;26:3639–44.
[30] Foster CM, Collazo R, Sitar Z, Ivanisevic A. Cell behavior on gallium nitride surfaces: peptide affinity attachment versus covalent functionalization. Langmuir 2013;29:8377–84.
[31] Jewett SA, Makowski MS, Andrews B, Manfra MJ, Ivanisevic A. Gallium nitride is biocompatible and non-toxic before and after functionalization with peptides. Acta Biomater 2012;8:728–33.
[32] Podolska A, Tham S, Hart RD, Seeber RM, Kocan M, Kocan M, et al. Biocompatibility of semiconducting AlGaN/GaN material with living cells. Sens Actuators B Chem 2012;169:401–6.
[33] Chen CR, Young TH. The effect of gallium nitride on long-term of neuritic function in cerebellar culture induced aging granule cells. Biomaterials 2008;29:1573–82.
[34] Foster CM, Collazo R, Sitar Z, Ivanisevic A. Aqueous stability of Ga- and N-polar gallium nitride. Langmuir 2013;29:216–20.
[35] Gupta S, Elias M, Wen XJ, Shapiro J, Brillson L, Lu W, et al. Detection of clinically relevant levels of protein analyte under physiologic buffer using planar field effect transistors. Biosens Bioelectron 2008;24:505–11.
[36] Diaz DJ, Williamson TL, Adesida I, Bohn PW, Molnar RJ. Morphology and luminescence of porous GaN generated via Pt-assisted electroless etching. J Vac Sci Technol B 2002;20:2375–83.
[37] Nie B, Duan BK, Bohn PW. Nanoporous Ag-GaN thin films prepared by metal-assisted electroless etching and deposition as three-dimensional substrates for surface-enhanced Raman scattering. J Raman Spectrosc 2012;43:1347–53.
[38] Chen CC, Yeh CC, Chen CH, Yu MY, Liu HL, Wu JJ, et al. Catalytic growth and characterization of gallium nitride nanowires. J Am Chem Soc 2001;123:2791–8.
[39] Goldberger J, He RR, Zhang YF, Lee SW, Yan HQ, Choi HJ, et al. Single-crystal gallium nitride nanotubes. Nature 2003;422:599–602.
[40] Makowski MS, Zemlyanov DY, Ivanisevic A. Olefin metathesis reaction on GaN (0001) surfaces. Appl Surf Sci 2011;257:4625–32.
[41] Makowski MS, Zemlyanov DY, Lindsey JA, Bernhard JC, Hagen EM, Chan BK, et al. Covalent attachment of a peptide to the surface of gallium nitride. Surf Sci 2011;605:1466–75.
[42] Estephan E, Larroque C, Bec N, Martineau P, Cuisinier FJG, Cloitre T, et al. Selection and mass spectrometry characterization of peptides targeting semiconductor surfaces. Biotechnol Bioeng 2009;104:1121–31.
[43] Liu WY, Zhang Y, Thomopoulos S, Xia YN. Generation of controllable gradients in cell density. Angew Chem Int Ed 2013;52:429–32.
[44] Liu H, Webster TJ. Nanomedicine for implants: a review of studies and necessary experimental tools. Biomaterials 2007;28:354–69.
[45] Yang R, Zhang Y, Li J, Han Q, Zhang W, Lu C, et al. Graphene oxide assisted synthesis of GaN nanostructures for reducing cell adhesion. Nanoscale 2013;5.
[46] Kotov NA, Winter JO, Clements IP, Jan E, Timko BP, Campidelli S, et al. Nanomaterials for neural interfaces. Adv Mater 2009;21:3970–4004.
[47] Makowski MS, Ivanisevic A. Molecular analysis of blood with micro-/nanoscale field-effect-transistor biosensors. Small 2011;7:1863–75.
[48] Dziecielewski I, Weyher JL, Dzwolak W. On the hydrophobicity of modified Ga-polar GaN surfaces. Appl Phys Lett 2013;102.
[49] Giamblanco N, Martines E, Marletta G. Laminin adsorption on nanostructures: switching the molecular orientation by local curvature changes. Langmuir 2013;29:8335–42.
[50] Han M, Sethuraman A, Kane RS, Belfort G. Nanometer-scale roughness having little effect on the amount or structure of adsorbed protein. Langmuir 2003;19:9868–72.
[51] Lord MS, Foss M, Besenbacher F. Influence of nanoscale surface topography on protein adsorption and cellular response. Nano Today 2010;5:66–78.
[52] Mita S, Collazo R, Rice A, Dalmau RF, Sitar Z. Influence of gallium supersaturation on the properties of GaN grown by metalorganic chemical vapor deposition. J Appl Phys 2008;104:013521.
[53] Dykstra MJ. Why 4F:1G fixative works for me. Microsc Today 2010;18:50–3.
[54] Castner DG, Ratner BD. Biomedical surface science: foundations to frontiers. Surf Sci 2002;500:28–60.
[55] Beighley R, Spedden E, Sekeroglu K, Atherton T, Demirel MC, Staii C. Neuronal alignment on asymmetric textured surfaces. Appl Phys Lett 2012;101.
[56] Hu W, Yim EKF, Reano RM, Leong KW, Pang SW. Effects of nanoimprinted patterns in tissue-culture polystyrene on cell behavior. J Vac Sci Technol B 2005;23:2984–9.
[57] Cai L, Zhang L, Dong JY, Wang SF. Photocured biodegradable polymer substrates of varying stiffness and microgroove dimensions for promoting nerve cell guidance and differentiation. Langmuir 2012;28:12557–68.
[58] Nomizu M, Weeks BS, Weston CA, Kim WH, Kleinman HK, Yamada Y. Structure–activity study of a laminin alpha-1 chain active peptide segment Ile-Lys-Val-Ala-Val (IKVAV). Febs Lett 1995;365:227–31.